Quantum Yields for Cl(^2P_j) Atom Formation from the Photolysis of Chlorofluorocarbons and Chlorinated Hydrocarbons at 193.3 nm

Fumikazu Taketani, Kenshi Takahashi,* and Yutaka Matsumi

Solar-Terrestrial Environment Laboratory and Graduate School of Science, Nagoya University, 3-13 Honohara, Toyokawa, Aichi 442-8507, Japan

Received: December 20, 2004; In Final Form: January 25, 2005

Cl($^2P_{3/2}$) and Cl*($^2P_{1/2}$) atoms produced from the photodissociation of chlorofluorocarbons (CFCs) and chlorinated hydrocarbons at 193.3 nm have been detected quantitatively by a technique of vacuum ultraviolet laser-induced fluorescence (VUV-LIF) spectroscopy at 135.2 and 134.7 nm for $j = {}^1/_2$ and ${}^3/_2$, respectively. The quantum yields for total Cl-atom formation in the 193.3 nm photolysis at 295 ± 2 K have been determined to be 1.03 ± 0.09, 1.01 ± 0.08, 1.03 ± 0.08, 1.03 ± 0.10, 1.41 ± 0.14, 1.02 ± 0.08, and 0.98 ± 0.08 for CF_2Cl_2, $CFCl_3$, CH_2Cl_2, $CHCl_3$, CCl_4, $CHFCl_2$, and CCl_3CF_3, respectively. Those results suggest that the single C−Cl bond rupture always occurs in the photolysis of these molecules except for CCl_4. Formation of two Cl atoms partly takes place in the photodissociation of CCl_4. The quantum yields for total Cl-atom formation in the 193.3 nm photolysis of $CHBr_2Cl$ and $CHBrClCF_3$ are 0.27 ± 0.02 and 0.28 ± 0.02, respectively, which suggests that the C−Br bond rupture is a main channel in the photodissociation processes. The branching ratios between the spin−orbit states, Cl*($^2P_{1/2}$) and Cl($^2P_{3/2}$), have also been determined for the photodissociation of the chlorinated compounds at 193.3 nm. The UV photodissociation processes giving rise to formation of Cl(^2P_j) atoms from the chlorinated compounds studied here have been discussed.

1. Introduction

Photochemical properties of halogen-containing compounds such as chlorofluorocarbons (CFCs) have been a matter of great importance from viewpoints of atmospheric chemistry[1−5] as well as physical chemistry. CFCs released in the troposphere are injected into the stratosphere where they are decomposed by photochemical processes initiated by sunlight absorption in the UV region between 190 and 220 nm. The chlorine atoms released from CFCs play crucial roles in the catalytic decomposition of stratospheric ozone. It is indispensable for assessment of their impacts on the global environment to estimate the primary product yields from the photolysis of halogen-containing compounds.

We have studied photodissociation processes of CF_2Cl_2, $CFCl_3$, CH_2Cl_2, $CHCl_3$, CCl_4, $CHFCl_2$, $CHBr_2Cl$, $CHBrClCF_3$, and CCl_3CF_3 at 193.3 nm in this work. The photoabsorption spectra of these chlorinated compounds are diffuse around 200 nm, which indicates that these molecules are dissociative in the excited states.[6] Energetically available pathways in the 193.3 nm photolysis of the chlorine compounds are listed in Table 1, where the values of the bond dissociation energies and heats of formation were taken from literatures.[4,5,7−11] The energetics for CCl_3CF_3 was not estimated, because the heat of formation of the parent molecule and the radical fragments are not available.

Felder and Demuth[12] studied laser photodissociation of $CFCl_3$ at 193.3 nm using a time-of-flight mass-spectrometry technique to measure the velocity distributions of the photofragments. They found that the distribution of the kinetic energy release for Cl-atom formation was very narrow and that the average kinetic energy release corresponded to 42% of the available energy. Their results suggest the exclusive dissociation to $CFCl_2$ + Cl, with the $CFCl_2$ fragment containing insufficient energy for prompt dissociation to produce a second Cl atom. Baum and Huber[13] studied laser photodissociation of CF_2Cl_2 at 193.3 nm using the same technique, and found that the situation was almost same as that for $CFCl_3$. The IUPAC subcommittee[4] recommends the quantum yield for Cl-atom formation from the photolysis of CF_2Cl_2 and $CFCl_3$ around 200 nm to be unity as inferred from these kinetic energy release measurements. However, the results of the kinetic energy release measurements are inconsistent with earlier quantitative measurements presented by Rebbert and Ausloos.[14] They photolyzed CF_2Cl_2 and $CFCl_3$ in the presence of CH_4 and C_2H_6 that were added as Cl-atom scavengers and analyzed the products quantitatively using a flame ionization gas chromatography technique. They concluded that formation of two Cl atoms occurred increasingly as the photolysis wavelength became shorter below 230 nm. Quantitative measurement of the quantum yields for Cl-atom formation in the 193.3 nm photolysis of CH_2Cl_2, $CHCl_3$, $CHFCl_2$, $CHBr_2Cl$, $CHBrClCF_3$, and CCl_3CF_3 have not been reported yet.

Predominance of the C−Cl bond cleavage in the 193.3 nm photolysis of $CHCl_3$ and $CHFCl_2$[15,16] was suggested by photofragment translational spectroscopy under molecular beam conditions. The primary H-atom formation yield from CH_2Cl_2 photolysis at 193.3 nm was determined to be (0.2 ± 0.1) × 10^{-2} by Brownsword et al.[17] They also reported that no significant H-atom formation in the photolysis of $CHCl_3$ was observed. Their results imply the predominant rupture of C−Cl bond in CH_2Cl_2 and $CHCl_3$ following 193.3 nm photoexcitation. For the photolysis of CCl_4, there are several experimental studies on the quantum yield for Cl-atom formation between 135 and 254 nm.[4,18] Hanf et al. have recently reported the primary Cl-atom quantum yield from CCl_4 at 193.3 nm to be 1.5 ± 0.1,[18] implying that substantial amounts of Cl atoms should be formed

* Corresponding author. E-mail: kent@stelab.nagoya-u.ac.jp.

10.1021/jp044218+ CCC: $30.25 © 2005 American Chemical Society
Published on Web 03/03/2005

TABLE 1: Energetically Possible Dissociation Pathways and Their Enthalpy Values for the Photolysis of the Chlorinated Compounds at 193.3 nm (Photon Energy: 147.9 kcal mol^{-1})

parent molecules	fragments	ΔH^a
$CFCl_3$	$CFCl_2 + Cl$	75.8
	$CFCl + 2Cl$	133.5
	$CFCl + Cl_2$	75.6
	$CCl_3 + F$	104.2
	$CCl_2 + FCl$	109.8
CF_2Cl_2	$CF_2Cl + Cl$	80.3
	$CF_2 + 2Cl$	132.0
	$CF_2 + Cl_2$	74.1
	$CF_2Cl + F$	115.8
	$CFCl + FCl$	112.2
$CHCl_3$	$CHCl_2 + Cl$	74.8
	$CHCl + 2Cl$	131.4
	$CHCl + Cl_2$	102.5
	$CCl_3 + H$	93.7
	$CCl_2 + HCl$	57.5
CH_2Cl_2	$CH_2Cl + Cl$	79.7
	$CHCl_2 + H$	96.1
	$CHCl + HCl$	78.6
	$CH_2(X^1A_1) + Cl_2$	116.0
	$CH_2(a^3B_1) + Cl_2$	125.0
$CHFCl_2$	$CHFCl + Cl$	82.5
	$CFCl_2 + H$	98.9
	$CCl_2 + HF$	57.8
	$CFCl + HCl$	53.5
	$CHCl + FCl$	132.7
$CHBr_2Cl$	$CHBrCl + Br$	58.8
	$CHBr_2 + Cl$	71.9
	$CBr_2Cl + H$	88.9
	$CHBr + Cl + Br$	142.6
	$CHCl + 2Br$	129.3
$CHBrClCF_3$	$CHClCF_3 + Br$	56.7
	$CHBrCF_3 + Cl$	68.7
	$CHClFCF_2 + Br$	74.3
	$CClCF_3(S) + HBr$	75.2
	$CClCF_3(T) + HBr$	78.9
	$CHBrFCF_2 + Cl$	87.7
	$CHFCF_2 + Br + Cl$	95.6
	$CHClCF_2 + Br + F$	120.6
	$CHBrCF_2 + Cl + F$	132.1
	$CHCF_3(T) + Br + Cl$	141.2

[a] Reaction enthalpy in units of kcal/mol (refs 4, 5, 7−11). For atomic halogen fragments, the values for the spin−orbit ground state $j = {}^3/_2$ was presented. The spin−orbit energy difference between $Cl(^2P_{3/2})$ and $Cl^*(^2P_{1/2})$ is 2.51 kcal/mol. For fragmentations from $CHBrClCF_3$, (T) and (S) stand for the triplet and singlet states, respectively.

via $CCl_2 + Cl + Cl$, although the IUPAC recommendation have suggested that the Cl quantum yield is unity in the range 174−275 nm.

The spin−orbit states of $Cl(^2P_{3/2})$ and $Cl^*(^2P_{1/2})$ are separated in energy by 2.51 kcal mol^{-1} (0.109 eV), with the $Cl^*(^2P_{1/2})$ state being higher in energy. Fine-structure branching ratios of atomic photoproducts should depend on both the nature of the photoprepared potential energy surfaces and subsequent nonadiabatic couplings between the surfaces as the products depart. The fine-structure branching ratios of $Cl(^2P_j)$ atoms produced in the photolysis of CFCs and chlorinated hydrocarbons at 193.3 nm were reported for CF_2Cl_2, $CFCl_3$, CH_2Cl_2, $CHCl_3$ and CCl_4 by Matsumi et al.,[19] using (2+1) resonance enhanced multiphoton ionization detection. Tunable diode laser probe[20] and LIF spectroscopy[18] was also utilized to measure the fine-structure branching ratio of $Cl(^2P_j)$ from CCl_4 photolysis at 193.3 nm. For the fine-structure branching ratios of $Cl(^2P_j)$ produced in the photolysis of $CHFCl_2$, $CHBr_2Cl$, $CHBrClCF_3$, and CCl_3CF_3, no literature data are available.

In this paper, we report the quantum yield for $Cl(^2P_j)$ atom formation in the 193.3 nm photolysis of the chlorine-containing molecules at 295 ± 2 K. The $Cl(^2P_j)$ atoms are detected quantum-state selectively using a technique of vacuum-ultraviolet laser-induced fluorescence (VUV-LIF). The absolute quantum yield values were determined by means of a photolytic calibration method using HCl photolysis as a reference source for well-defined $Cl(^2P_j)$ concentrations. The branching ratios among the spin−orbit states of $Cl(^2P_j)$ are also determined. Photodissociation processes of the CFCs and chlorinated hydrocarbons to generate $Cl(^2P_j)$ atoms at 193.3 nm are discussed.

2. Experimental Section

Experiments were conducted using the laser flash photolysis/laser-induced fluorescence apparatus, which was almost the same as in the previous studies.[21,22] The reactant gases were flowed into the reaction cell that was continuously evacuated by a rotary pump. An ArF excimer laser (Lambda Physik, COMPex 102) was used as a photolysis light source. The typical pulse energy was 3 mJ, which was measured by a calorimeter (Scientech, AC50UV). The $Cl(^2P_{3/2})$ and $Cl^*(^2P_{1/2})$ photofragments were detected using the VUV-LIF technique at 134.7 nm ($4s^2P_{3/2} \rightarrow 3p^2P_{3/2}$) and 135.2 nm ($4s^2P_{1/2} \rightarrow 3p^2P_{1/2}$), respectively. The tunable VUV light was generated by two-photon resonance four-wave mixing in Kr gas,[23,24] using two dye lasers pumped by a single XeCl excimer laser (Lambda Physik, COMPex 201, FL3002 and Scanmate 2). The laser system was operated at 10 Hz repetition rate. The delay time between the photolysis and probe laser pulses was typically set to 100 ns.

In the quantum yield measurements, the chlorinated compound (CF_2Cl_2, $CFCl_3$, CH_2Cl_2, $CHCl_3$, CCl_4, $CHFCl_2$, $CHBr_2Cl$, $CHBrClCF_3$, and CCl_3CF_3) and HCl was photolyzed alternatively. The photodissociation of HCl at 193.3 nm generates the $Cl(^2P_j)$ fragments with the fine-structure branching ratio of 0.59:0.41 for $j = {}^3/_2:{}^1/_2$.[25,26] The photolysis and probe laser beams crossed at right angles in the reaction chamber. The LIF of $Cl(^2P_j)$ was detected by a solar-blind photomultiplier tube (PMT) (EMR, 541J-08-17). The PMT had a LiF window and a KBr photocathode, which was sensitive only in the wavelength region between 105 and 150 nm. The output from the PMT was preamplified and fed into a gated integrator (Stanford Research, SR-250).

The typical pressures were 2.8−16.1 and 18−45 mTorr for chlorinated compounds and HCl, respectively. The reaction rate coefficients for the reactions of Cl-atom with the chlorinated compounds studied here are smaller than 2.0×10^{-14} cm^3 molecule^{-1} s^{-1}.[5] The decay rate coefficients of $Cl^*(^2P_{1/2})$ in collisions with the chlorinated compounds range from 1.2×10^{-11} to 2.2×10^{-10} cm^3 molecule^{-1} s^{-1}.[27] Therefore, under our experimental conditions, the chemical loss of $Cl(^2P_{3/2})$ and $Cl^*(^2P_{1/2})$ is negligibly small during the delay time between the photolysis and probe laser pulses. The reagents were obtained commercially and the suppliers stated that the purities of CF_2Cl_2, $CFCl_3$, CH_2Cl_2, $CHCl_3$, CCl_4, $CHFCl_2$, $CHBr_2Cl$, $CHBrClCF_3$, and CCl_3CF_3 were 99.8, 99, 99, 98, 99.8, 99, 95, 99, and 99%, respectively. Those reagents were used in the experiments without further purification.

3. Results

Figure 1 shows fluorescence excitation spectra of nascent $Cl(^2P_{3/2})$ and $Cl^*(^2P_{1/2})$ atoms produced from (a) $CFCl_3$, CF_2Cl_2, CH_2Cl_2 $CHCl_3$, and CCl_4 and (b) $CHFCl_2$, $CHBr_2Cl$, $CHBrClCF_3$, and CCl_3CF_3 photolysis at 193.3 nm, where the wavelength of the probe laser was scanned across the resonance

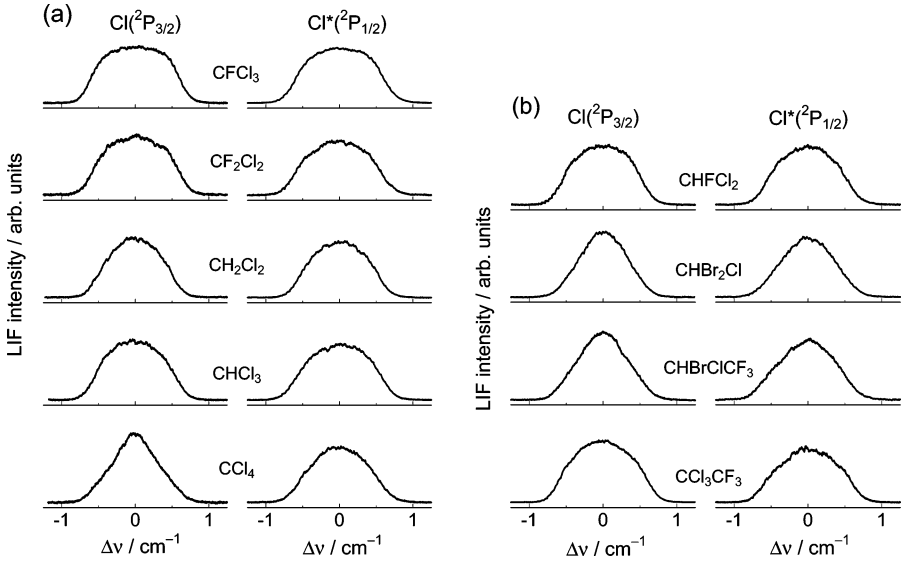

Figure 1. Fluorescence excitation spectra of nascent $Cl(^2P_{3/2})$ and $Cl^*(^2P_{1/2})$ atoms produced from (a) $CFCl_3$, CF_2Cl_2, CH_2Cl_2 $CHCl_3$, and CCl_4 and (b) $CHFCl_2$, $CHBr_2Cl$, $CHBrClCF_3$, and CCl_3CF_3 photolysis at 193.3 nm.

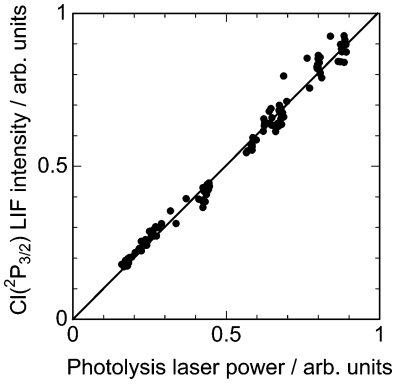

Figure 2. LIF signal intensity of $Cl(^2P_{3/2})$ versus 193.3 nm laser intensity. $CFCl_3$ (4.4 mTorr) was photolyzed at 193.3 nm and the $Cl(^2P_{3/2})$ atoms produced were detected directly using the VUV-LIF technique. The delay time between the pump and probe laser pulses was 100 ns. The straight line indicates the result of linear least-squares fit analysis of the data measured.

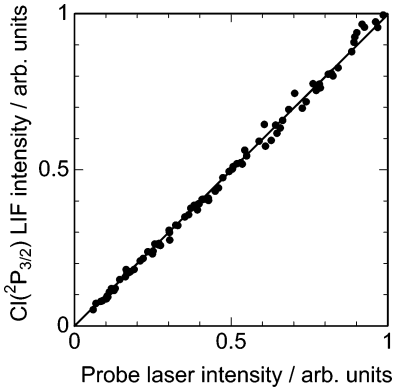

Figure 3. LIF signal intensity of $Cl(^2P_{3/2})$ versus probe laser intensity. $CFCl_3$ (4.4 mTorr) was photolyzed at 193.3 nm and the $Cl(^2P_{3/2})$ atom produced was detected directly using the VUV-LIF technique. The delay time between the pump and probe laser pulses was 100 ns. The intensity of the VUV laser was controlled by changing the Kr gas pressure in the frequency conversion cell between 0.2 and 20 Torr, while keeping the photolysis laser power constant.

frequencies of the $4s^2P_{3/2} \rightarrow 3p^2P_{3/2}$ and $4s^2P_{1/2} \rightarrow 3p^2P_{1/2}$ transitions. Figure 2 shows the linear dependence of LIF signal intensity for $Cl(^2P_{3/2})$ atoms produced from $CFCl_3$ on the photolysis laser power. For $Cl^*(^2P_{1/2})$ photoproducts, the linear dependence of LIF signal on the photolysis laser power was also observed. No significant LIF signal of $Cl(^2P_{3/2})$ and $Cl^*(^2P_{1/2})$ was observed when the photolysis laser was turned off under our experimental conditions. Figure 3 shows the linear dependence of the $Cl(^2P_{3/2})$ LIF signal intensity on the VUV probe laser power at 134.7 nm, in which relative intensity of the VUV laser was varied by changing the Kr gas pressure. Those results indicate that multiphoton absorption of $CFCl_3$ at 193 nm can be safely ignored and neither photolysis of parent molecule nor primarily formed radical species at 134 nm was significant under our experimental conditions. The similar results were obtained for the $Cl^*(^2P_{1/2})$ formation from the photolysis of $CFCl_3$.

The quantum yields of $Cl(^2P_{3/2})$ and $Cl^*(^2P_{1/2})$ atoms, Φ_{Cl} and Φ_{Cl^*}, from the 193.3 nm photolysis of chlorinated compounds were determined from the LIF signal intensities of $Cl(^2P_{3/2})$ and $Cl^*(^2P_{1/2})$. The absolute values of the quantum yield of $Cl(^2P_{3/2})$ and $Cl^*(^2P_{1/2})$ atoms were calibrated by the LIF intensity of Cl atoms from the photolysis of HCl at 193.3 nm. Using the literature values of $\Phi_{Cl} = 0.59$ and $\Phi_{Cl^*} = 0.41$ for HCl photolysis,[25,26] the values of Φ_{Cl} and Φ_{Cl^*} for chlorinated compounds were calculated from the following expressions:

$$\Phi_{Cl} = \frac{S_{Cl}{}^{M}\sigma^{HCl}[HCl]}{S_{Cl}{}^{HCl}\sigma^{M}[M]} \times 0.59 \quad (1)$$

$$\Phi_{Cl^*} = \frac{S_{Cl^*}{}^{M}\sigma^{HCl}[HCl]}{S_{Cl^*}{}^{HCl}\sigma^{M}[M]} \times 0.41 \quad (2)$$

$S_{Cl}{}^{M}$ and $S_{Cl}{}^{HCl}$ are the peak areas of the fluorescence excitation spectra of $Cl(^2P_{3/2})$ produced from the photolysis of parent molecule M and HCl at 193.3 nm, respectively. Similarly, $S_{Cl^*}{}^{M}$ and $S_{Cl^*}{}^{HCl}$ are those for $Cl^*(^2P_{1/2})$. [M] and [HCl] are the number densities of M and HCl in the photolysis cell, respectively. σ^{M} and σ^{HCl} are the room-temperature photoabsorption cross-sections of M and HCl at 193.3 nm, respectively. The values of the absorption cross-sections of HCl, CF_2Cl_2, $CFCl_3$, CH_2Cl_2, $CHCl_3$, CCl_4 and $CHFCl_2$ at 193.3 nm were taken from the literature,[5,28] which were 8.69×10^{-20}, $3.65 \times$

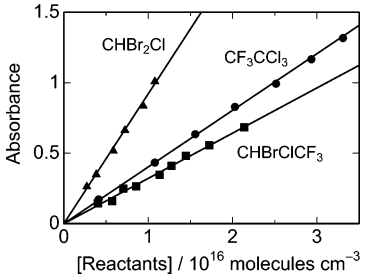

Figure 4. Beer−Lambert plots for photoabsorption of $CHBr_2Cl$, $CHBrClCF_3$, and CCl_3CF_3 at 193.3 nm. The straight lines indicate the results from the linear least-squares analysis of the absorbance measurements.

TABLE 2: Quantum Yields for Production of Cl($^2P_{3/2}$) and Cl*($^2P_{1/2}$) Atoms in the Photolysis of Chlorinated Compounds at 193.3 nm[a]

compound	Cl($^2P_{3/2}$)	Cl*($^2P_{1/2}$)	total[b]
CF_2Cl_2	0.77 ± 0.09	0.26 ± 0.03	1.03 ± 0.09
$CFCl_3$	0.67 ± 0.07	0.34 ± 0.04	1.01 ± 0.08
CH_2Cl_2	0.69 ± 0.07	0.34 ± 0.04	1.03 ± 0.08
$CHCl_3$	0.78 ± 0.09	0.25 ± 0.04	1.03 ± 0.10
CCl_4	0.96 ± 0.12	0.45 ± 0.07	1.41 ± 0.14
$CHFCl_2$	0.85 ± 0.07	0.17 ± 0.02	1.02 ± 0.08
$CHBr_2Cl$	0.18 ± 0.02	0.09 ± 0.01	0.27 ± 0.02
$CHBrClCF_3$	0.23 ± 0.02	0.05 ± 0.01	0.28 ± 0.02
CCl_3CF_3	0.87 ± 0.09	0.11 ± 0.01	0.98 ± 0.08

[a] The quoted errors include the 2σ statistical deviations in the LIF intensity measurements and the uncertainties of the literature values of Φ_{Cl} and Φ_{Cl^*} for HCl. [b] Sum of the quantum yield values for production of Cl($^2P_{3/2}$) and Cl*($^2P_{1/2}$) atoms.

10^{-19}, 1.36×10^{-18}, 3.35×10^{-19}, 7.90×10^{-19}, 8.68×10^{-19} and 2.15×10^{-19} cm^2 molecule^{-1}, respectively. Because the values for absorption cross-sections of $CHBr_2Cl$, $CHBrClCF_3$, and CCl_3CF_3 at 193.3 nm were not reported before, they have been measured in the present study. Beer−Lambert plots of photoabsorption of the three species at 193.3 nm are shown in Figure 4. All the measurements were performed at 295 ± 2 K. The cross-section values obtained are $(3.04 \pm 0.19) \times 10^{-18}$, $(1.07 \pm 0.07) \times 10^{-18}$, and $(1.34 \pm 0.07) \times 10^{-18}$ cm^2 molecule^{-1}, for $CHBr_2Cl$, $CHBrClCF_3$ and CCl_3CF_3, respectively.

Table 2 lists the values of Φ_{Cl} and Φ_{Cl^*} obtained from the 193.3 nm photolysis of the chlorine compounds. The quoted errors include the 2-sigma statistical deviations in the LIF intensity measurements and the uncertainties of the literature values of Φ_{Cl} and Φ_{Cl^*} for HCl. Experimental runs of the LIF intensity measurements for the 193.3 nm photolysis of M and HCl were performed alternatively 10 to 15 times for each chlorinated compound (M). Table 3 lists the values of the nascent fine-structure branching ratio, $[Cl^*(^2P_{1/2})]/([Cl^*(^2P_{1/2})] + [Cl(^2P_{3/2})])$, in the photolysis of the chlorinated compounds at 193.3 nm.

4. Discussion

CF_2Cl_2, $CFCl_3$, CH_2Cl_2, $CHCl_3$ and $CHFCl_2$. The values of the quantum yield for the total chlorine formation, $\Phi_{Cl} + \Phi_{Cl^*}$, are almost unity within the uncertainties for CF_2Cl_2, $CFCl_3$, CH_2Cl_2, $CHCl_3$ and $CHFCl_2$, as listed in Table 2. This suggests that single C−Cl bond rupture occurs mainly in the photolysis of those molecules at 193.3 nm. Our results of the quantitative measurements using the LIF detection for Cl atoms from CF_2Cl_2, $CFCl_3$, $CHCl_3$ and $CHFCl_2$ are consistent with the experimental observations using the time-of-flight mass spectrometry for the kinetic energy distributions of the photofragments from those molecules.[12,13,15] Slow components of chlorine atoms due to the three-body dissociation producing two Cl atoms were not detected in the photodissociation of CF_2Cl_2,[13] $CFCl_3$,[12] $CHCl_3$ and $CHFCl_2$.[15] The earlier measurements of the Cl-atom formation yields for the photolysis of CF_2Cl_2 and $CFCl_3$ by Rebbert and Ausloos[14] indicated that formation of two Cl atoms occurs increasingly as the photolysis wavelength becomes shorter below 230 nm, which disagrees with our results. The reason for the disagreement is not clear here. We have directly detected the product Cl($^2P_{3/2}$) and Cl*($^2P_{1/2}$) atoms using the VUV-LIF technique, whereas Rebbert and Ausloos measured the product concentrations from the reactions of photofragment Cl-atom with scavenger molecules (CH_4 and C_2H_6) using a gas chromatography technique.

TABLE 3: Nascent Fine-structure Branching Ratios of the Chlorine Atoms Produced in the Photolysis of Chlorinated Compounds at 193.3 nm

	$[Cl^*(^2P_{1/2})]/[Cl^*(^2P_{1/2})] + [Cl(^2P_{3/2})]$	
compound	this work[a]	ref
CF_2Cl_2	0.25 ± 0.04	0.24 ± 0.03[b]
$CFCl_3$	0.34 ± 0.04	0.29 ± 0.08[b]
CH_2Cl_2	0.33 ± 0.04	0.26 ± 0.05[b]
$CHCl_3$	0.24 ± 0.04	0.26 ± 0.05[b]
CCl_4	0.32 ± 0.05	0.29 ± 0.10[b]
$CHFCl_2$	0.17 ± 0.02	
$CHBr_2Cl$	0.33 ± 0.05	
$CHBrClCF_3$	0.18 ± 0.02	
CCl_3CF_3	0.11 ± 0.02	

[a] The quoted errors include the 2σ statistical deviations in the LIF intensity measurements and the uncertainties of the literature values of Φ_{Cl} and Φ_{Cl^*} for HCl. [b] Taken from the paper published by Matsumi et al.[19] but modified as follows. Matsumi et al.[19] presented the fine-structure branching ratios from the photolysis of the chlorinated compounds, using the value of $[Cl^*(^2P_{1/2})]/([Cl^*(^2P_{1/2})] + [Cl(^2P_{3/2})]) = 0.33 \pm 0.03$ [refs 31−33] for the photodissociation of HCl at 193.3 nm as a standard. The values indicated in this table have been rescaled with the recent value of 0.41 ± 0.01 presented by Zhang et al.[25] for the photolysis of HCl at 193.3 nm.

The stratospheric ozone destruction is initiated by formation of Cl atoms in the photolysis of CFCs such as CF_2Cl_2, $CFCl_3$ and $CHFCl_2$.[1−3] The effective wavelengths for the photolysis of these molecules are shorter than 220 nm due to the spectral overlaps between the photoabsorption spectra of the CFC molecules and the solar actinic flux in the atmosphere. As obtained in this study, one Cl-atom is produced from the photolysis of CFCs. In the atmosphere, for example, the CF_2Cl radical produced from CF_2Cl_2 photolysis recombines rapidly with O_2 molecules, and the peroxy radical CF_2ClO_2 formed reacts with NO or RO_2 ($RO_2 = HO_2$ and other peroxyradicals) to form CF_2ClO radical. The atmospheric fate of the CF_2ClO radical was studied experimentally[29] and theoretically,[30] in which the decomposition products of Cl atom and CF_2O were identified. Finally, two Cl atoms are produced and participate in the cycle reactions for catalytic destruction of the stratospheric ozone, following the initial photodissociation process of CF_2Cl_2.

Matsumi et al.[19] reported the nascent fine-structure branching ratios of Cl($^2P_{3/2}$) and Cl*($^2P_{1/2}$) atoms produced from the 193.3 nm photolysis of several chlorine containing molecules, using the REMPI detection of the Cl(^2P_j) fragments around 235 nm. They presented the fine-structure branching ratios from the photolysis of the chlorinated compounds, using the value of $[Cl^*(^2P_{1/2})]/([Cl^*(^2P_{1/2})] + [Cl(^2P_{3/2})]) = 0.33 \pm 0.03$[31−33] for the photodissociation of HCl at 193.3 nm as a standard. The values listed in Table 3 as references have been rescaled with

the recent value of 0.41 ± 0.01 presented by Zhang et al.[25] for the photodissociation of HCl at 193.3 nm. Our results of the fine-structure branching ratios are in good agreement with those obtained by Matsumi et al., as listed in Table 3. The fine-structure branching ratios of Cl atoms produced from the vibrationally meditated photodissociation of CH_2Cl_2 and CHF_2Cl molecules with near-infrared (∼1151 nm) and ultraviolet (∼235 nm) laser light have been studied.[34,35]

The photoabsorption band of CFCs and chlorinated hydrocarbons around 193.3 nm has no structure, indicating that the excited state is dissociative. The absorption of a 193.3 nm photon by chloromethanes leads to an excitation to the first absorption band which originates from a $3p\pi \rightarrow \sigma^*$(C−Cl) transition within the valence shell, where $3p\pi$ is the lone pair orbital of Cl and σ^* is the antibonding orbital of the C−Cl bond.[6,36−38] Therefore, it is expected that the initial excitation is localized in the C−Cl bond leading predominantly to the breaking of this bond. The set of upper states of the $3p\pi \rightarrow \sigma^*$ transitions of the first absorption band of CFCs and chlorinated hydrocarbons includes five states $^1Q_2$, $^3Q_1$, $^3Q_0^+$, $^3Q_0^-$, and $^1Q_1$ as designated by Mulliken,[39] and three of which ($^3Q_1$, $^3Q_0^+$ and $^1Q_1$) have dipole-allowed transitions from the ground state. The $^3Q_0^+$ state correlates adiabatically with Cl*($^2P_{1/2}$) products, whereas the $^3Q_1$ and $^1Q_1$ states do with Cl($^2P_{3/2}$) products.

The observed branching ratios of the chlorine fine-structure levels in the photodissociation may be ruled by the nonadiabatic transition among the excited-state potential curves and/or by the nature of the excited state(s). The probability of the nonadiabatic transition depends on (a) the strength of the spin−orbit, (b) the Coriolis interactions, and (c) the relative velocities at the crossing point. At large nuclear distances, the adiabatic potentials asymptotically become degenerate with the free atom energies that are split by 2.51 kcal mol^{-1}. When the kinetic speed of the separating atoms is high enough, nonadiabatic transitions among the electronic states can take place. It can be seen in Table 3 that the values of the fine-structure branching ratio for the molecules which contain more chlorine atoms are larger than those for the molecules which contain less chlorine atoms. The reason for this tendency is not clear.

CCl_4. Rowe and Gedanken[40] assigned the *A* band of CCl_4 at 165−195 nm to $3a_1 \leftarrow 3t_2$, where the $3a_1$ and $3t_2$ molecular orbitals have $3p\sigma^*$ and $3p\pi$ characteristics, respectively. The IUPAC subcommittee recommends the total quantum yield for Cl($^2P_{3/2}$) and Cl*($^2P_{1/2}$) atom formation at 298 K to be unity in the range 174−225 nm. However, Hanf et al.[18] has shown that the total chlorine yield is 1.5 ± 0.1, which is close to the value of 1.41 ± 0.14 determined in this study. Formation of CCl_2 radical in the photolysis of CCl_4 at 193.3 nm has been observed,[41,42] which is consistent with the Cl-atom formation yield larger than 1. Production of two Cl atoms is significant in the photodissociation processes of CCl_4 at 193.3 nm. Hanf et al.[18] reported that the yields of 1.10 ± 0.05 and 0.40 ± 0.02 for Cl($^2P_{3/2}$) and Cl*($^2P_{1/2}$), respectively, in the photolysis of CCl_4 at 193.3 nm, which correspond to the fine-structure branching ratio of 0.27 ± 0.02 for [Cl*($^2P_{1/2}$)]/([Cl*($^2P_{1/2}$)] + [Cl($^2P_{3/2}$)]). The value of the fine-structure branching ratio presented by Hanf et al.[18] is in agreement with our result (0.32 ± 0.05) within the uncertainties.

Figure 1a shows fluorescence excitation spectra of nascent Cl($^2P_{3/2}$) and Cl*($^2P_{1/2}$) atoms produced from $CFCl_3$, CF_2Cl_2, CH_2Cl_2 $CHCl_3$, and CCl_4 photolysis at 193.3 nm. The spectral shape of Cl($^2P_{3/2}$) from CCl_4 is significantly different from those from $CFCl_3$, CF_2Cl_2, CH_2Cl_2 and $CHCl_3$ which produces only one chlorine atom primarily in the photolysis, whereas that of Cl*($^2P_{1/2}$) from CCl_4 has a similar shape to those from the other chlorinated compounds. The Cl($^2P_{3/2}$) spectrum from CCl_4 has narrow components around the resonance center, which corresponds to the Cl atoms having relatively slow velocities. The slow velocity components may come from the two Cl-atom elimination in the photolysis of CCl_4 at 193.3 nm, because the available energy for the two Cl-atom formation process is small, as listed in Table 1. The spectral shapes and quantum yields obtained for Cl($^2P_{3/2}$) and Cl*($^2P_{1/2}$) from CCl_4 suggest that the second Cl-atoms produced from the photolysis of CCl_4 preferably are in the $^2P_{3/2}$ state.

There are two possible mechanisms for two Cl-atom elimination in the photolysis of CCl_4. One is a parallel formation mechanism:

$$CCl_4 + h\nu\ (193.3\text{nm}) \rightarrow Cl + CCl_3 \qquad (3a)$$

$$CCl_4 + h\nu\ (193.3\text{nm}) \rightarrow 2Cl + CCl_2 \qquad (3b)$$

where the CCl_4 is excited to two different electronic excited states by the photoabsorption, and one of the states produces a single fast Cl-atom whereas the other state produces two slow Cl atoms.

The other mechanism is a sequential one:

$$CCl_4 + h\nu\ (193.3\text{nm}) \rightarrow Cl + CCl_3^* \qquad (4a)$$

$$CCl_3^* \rightarrow Cl + CCl_2 \qquad (4b)$$

where the CCl_3* radicals have enough energy to undergo the decomposition producing the second slow Cl atom. Because the total Cl-atom yield is 1.4, the yields for (3a) and (3b) should be 0.6 and 0.8 for the parallel mechanism, respectively, and the yields for (4a) and (4b) should be 1.0 and 0.4 for the sequential mechanism, respectively. From the spectral shape of Cl($^2P_{3/2}$) for CCl_4 in Figure 1a, the contribution of the slow Cl-atom is estimated to be about 40−50% of the total Cl formation. It is likely that the sequential mechanism can account for the Φ_{Cl} and Φ_{Cl^*} values observed.

$CHBr_2Cl$. The UV absorption spectra of $CHBr_2Cl$ at atmospheric temperatures were measured by Bilde et al.,[43] and two absorption bands are apparent, one maximizing near 205 nm and the other near 240 nm. As is analogous to CH_2BrCl[44] and CH_3Br,[45] the peak near 205 nm is assigned to the promotion of a nonbonding electron on the Br atom to an antibonding σ^* orbital on the C−Br bond. There has been experimental studies on the photodissociation of CH_2BrCl in UV region.[46−49] In the range 248−262 nm CH_2BrCl undergoes exclusively C−Br bond rupture, whereas in the range 193−242 nm it does predominantly C−Br bond rupture with a minor contribution of C−Cl bond rupture. A computational study at the MS−CASPT2 level of theory suggested that the lowest states corresponding to n(Br) $\rightarrow \sigma^*$(C−Br) and n(Cl) $\rightarrow \sigma^*$(C−Cl) transitions in CH_2BrCl appear at 6.1 eV(203 nm) and 7.2 eV(173 nm) in energy, respectively.[50] It is likely that the situations of $CHBr_2Cl$ are analogous to the photodissociation processes of CH_2BrCl in the UV region. Our present study has shown that the Cl-atom formation from the photolysis of $CHBr_2Cl$ at 193.3 nm occurs with the total Cl quantum yield $\Phi_{Cl} + \Phi_{Cl^*} = 0.27 \pm 0.02$, which implies that the C−Br bond rupture should be more significant than the C−Cl bond rupture. The spectral shape of Cl($^2P_{3/2}$) from the 193.3 nm photodissociation of $CHBr_2Cl$ has narrow components, as shown Figure 1b, which implies that the rupture of both C−Br and C−Cl bonds in the photodisso-

ciation takes places, that is, CHBr + Br + Cl. The wide components in the excitation spectra for $Cl(^2P_{3/2})$ and $Cl^*(^2P_{1/2})$ from $CHBr_2Cl$ suggest that the single C−Cl bond rupture giving rise to the $CHBr_2$ + Cl products also takes place.

$CHBrClCF_3$. The absorption spectra of $CHBrClCF_3$ at atmospheric temperatures in the wavelength range longer than 200 nm were reported by two groups,[43,51] and they are in good agreement with each other within 10% between 200 and 290 nm. The spectrum reported shows a maximum near 205 nm and decreases in roughly exponential fashion to longer wavelengths. The absorption spectrum has no significant vibrational structure in the UV region, suggesting that the electronic excited state is dissociative. In the photodissociation of $CHBrClCF_3$ at 193.3 nm, there are 10 energetically possible channels, and three of which produces Cl atom, as listed in Table 1. The total Cl-atom yield value obtained in the present study is 0.28 ± 0.02, implying that the rupture of the C−Br bond that is weaker than the C−Cl bond should be dominant following the 193.3 nm excitation. It is likely that the photoprepared state at 193.3 nm is primarily characterized as the $n(Br) \rightarrow \sigma^*(C-Br)$ transition, which results in the predominant rupture of C−Br bond. The photodissociation of $CHBrClCF_3$ at 157.6 nm was studied by Yokoyama et al.,[11] and the product channels $CHBrCF_3$ + Cl and $CHCF_3$ + Br + Cl were observed for Cl-atom formation. At 193.3 nm, as is analogous to 157.6 nm, it is likely that the $CHBrCF_3$ + Cl channel is responsible for the wide components in the excitation spectrum of $Cl(^2P_{3/2})$ from $CHBrCF_3$ shown in Figure 1b. The narrow components are attributable to the $CHCF_3$ + Br + Cl channel.

CCl_3CF_3. The absorption cross-section of CCl_3CF_3 at 193.3 nm has been measured to be $(1.34 \pm 0.07) \times 10^{-18}$ cm^2 molecule^{-1} at 295 ± 2 K in this work. The absorption cross-section of CF_3CF_2Cl (CFC-115) at 194 nm is reported to be 0.13×10^{-18} cm^2 molecule^{-1} at 295 K.[4,5] Because the chlorination of the fluorinated methanes and ethanes causes a red shift of their absorption spectra in general,[6] it is reasonable that the cross-section of CCl_3CF_3 at 193.3 nm is larger than that of CF_3CF_2Cl at 194 nm. The value of the total Cl-atom yield $\Phi_{Cl} + \Phi_{Cl^*} = 0.98 \pm 0.08$ obtained in this work indicates that the C−Cl bond rupture occurs predominantly in the photolysis of CCl_3CF_3 at 193.3 nm.

Acknowledgment. This work was supported in part by the Grant-in-Aids from the Ministry of Education, Sports, Culture and Science, Japan. The research grant for Dynamics of the Sun-Earth-Life Interactive System, No. G-4, the 21st Century COE Program from the Ministry is also acknowledged. This work was also supported in part by the Sumitomo Foundation and the Steel Industrial Foundation for the Advancement of Environmental Protection Technology.

References and Notes

(1) World Meteorological Organization. *Scientific Assessment of Ozone Depletion: 2002*, Global Ozone Research and Monitoring Project, Report No. 47, 2003.

(2) Finlayson-Pitts B. J.; Pitts, J. N., Jr. *Chemistry of the Upper and Lower Atmosphere, Theory, Experiments, and Applications*; Academic Press: New York, 2000.

(3) Wayne, R. P. *Chemistry of Atmospheres*, 3rd ed.; Oxford University Press: Oxford, NY, 2000.

(4) Atkinson, R.; Baulch, D. L.; Cox, R. A.; Crowley, J. N.; Hampson, R. F., Jr.; Kerr, J. A.; Rossi, M. J.; Troe, J. *Summary of Evaluated Kinetics and Photochemical Data for Atmospheric Chemistry, IUPAC Subcommittee on Gas Kinetics Data Evaluation for Atmospheric Chmistry*; Web Version (http://www.iupac-kinetic.ch.cam.ac.uk/), December 2002.

(5) Sander, S. P.; Friedl, R. R.; Golden, D. M.; Kurylo, M. J.; Huie, R. E.; Orkin, V. L.; Moortgat, G. K.; Ravishankara, A. R.; Kolb, C. E.; Molina, M. J.; Finlayson-Pitts, B. J. *Chemical Kinetics and Photochemical Data for use in Atmospheric Studies*, Evaluation No. 14, JPL Publication 02-25, 2003.

(6) Robin, M. B. *Higher excited states of polyatomic molecules*; Academic Press: New York, 1974; Vol. 1.

(7) Ibuki, T.; Hiraya, A.; Shobatake, K. *J. Chem. Phys.* **1992**, *96*, 8793.

(8) Seetula, J. A. *Phys. Chem. Chem. Phys.* **2000**, *2*, 3807.

(9) Seetula, J. A. *Phys. Chem. Chem. Phys.* **2003**, *5*, 849.

(10) Born, M.; Ingemann, S.; Nibbering, N. M. M. *J. Am. Chem. Soc.* **1994**, *116*, 7210.

(11) Yokoyama, A.; Yokoyama, K.; Takayanagi, T. *J. Phys. Chem. A* **1997**, *101*, 6647.

(12) Felder, P.; Demuth, C. *Chem. Phys. Lett.* **1993**, *208*, 21.

(13) Baum, G.; Huber, R. J. *Chem. Phys. Lett.* **1993**, *203*, 261.

(14) Rebbert, R. E.; Ausloos, P. J. *J. Photochem.* **1975**, *4*, 419.

(15) Yang, X.; Felder, P.; Huber, J. R. *Chem. Phys.* **1994**, *189*, 127.

(16) Naxhbor, M. D.; Giese, C. F.; Gentry, W. R. *J. Phys. Chem.* **1995**, *99*, 15400.

(17) Brownsword, R. A.; M. Hillenkamp, M.; Laurent, T.; Vatsa, R. K.; Volpp, H. R.; Wolfrum, J. *J. Phys. Chem.* **1997**, *101*, 5222.

(18) Hanf, A.; Läuter, A.; Volpp, H.-R. *Chem. Phys. Lett.* **2003**, *368*, 445.

(19) Matsumi, Y.; Tonokura, K.; Kawasaki, M.; Inoue, G.; Satyapal, S.; Bersohn, R. *J. Chem. Phys.* **1992**, *97*, 5261.

(20) Park, J.; Lee, Y.; Flynn, G. W. *Chem. Phys. Lett.* **1991**, *186*, 441.

(21) Matsumi, Y.; Izumi, K.; Skorokhodov, V.; Kawasaki, M.; Tanaka, N. *J. Phys. Chem. A* **1**997, *101*, 1216.

(22) Hitsuda, K.; Takahashi, K.; Matsumi, Y.; Wallington, T. J. *J. Phys. Chem. A* **2001**, *105*, 5131.

(23) Hilber, G.; Lago, A.; Wallenstein, R. *J. Opt. Soc. Am. B* **1987**, *4*, 1753.

(24) Marangos, J. P.; Shen, N.; Ma, H.; Hutchinson, M. H. R.; Connerade, J. P. *J. Opt. Soc. Am. B* **1990**, *7*, 1254.

(25) Zhang, J.; Dulligan, M.; Wittig, C. *J. Chem. Phys.* **1997**, *107*, 1403.

(26) Brownsword, R. A.; Schmiechen, P.; Volpp, H.-R.; Upadhyaya, H. P.; Jung, Y. J.; Jung, K.-H. *J. Chem. Phys.* **1999**, *110*, 11823.

(27) Chichinin, A. I. *J. Chem. Phys.* **2000**, *112*, 3772.

(28) Simon, P. C.; Gllootay, D.; Vanlaethem-Meuree, N.; Wisemberg, J. *J. Atmos. Chem.* **1988**, *7*, 107.

(29) Carr, R. W., Jr.; Peterson, D. G.; Smith, F. K. *J. Phys. Chem.* **1986**, *90*, 607.

(30) Drougas, E.; Kosmas, A. M.; Jalbout, A. F. *J. Phys. Chem. A* **2004**, *108*, 5972.

(31) Tiemann, E.; Kanamori, H.; Hirota, E. *J. Chem. Phys.* **1988**, *88*, 2457.

(32) Park, J.; Lee, Y.; Flynn, G. W. *Chem. Phys. Lett.* **1992**, *192*, 138.

(33) Tonokura, K.; Matsumi, Y.; Kawasaki, M.; Tasaki, S.; Bersohn, R. *J. Chem. Phys.* **1992**, *97*, 8210.

(34) Dorfman, G.; Melchior, A.; Rosenwaks, S.; Bar, I. *J. Phys. Chem. A* **2002**, *106*, 8285.

(35) Marom, R.; Golan, A.; Rosenwaks, S.; Bar, I. *Chem. Phys. Lett.* **2003**, *378*, 305.

(36) Ying, J. F.; Leung, K. T. *J. Chem. Phys.* **1994**, *101*, 8333.

(37) Ying, J. F.; Leung, K. T. *Phys. Rev. A* **1996**, *53*, 1476.

(38) Ying, J. F.; Leung, K. T. *J. Chem. Phys.* **1996**, *105*, 2188.

(39) Mulliken, R. S. *J. Chem. Phys.* **1935**, *3*, 513.

(40) Rowe, M. D.; Gedanken, A. *Chem. Phys.* **1975**, *10*, 1.

(41) Tiee, J. J.; Wampler, F. B.; Rice, W. W. *J. Chem. Phys.* **1980**, *72*, 2925.

(42) Shestov, A. A.; Kostina, S. A.; Shafir, E. V. *Chem. Phys. Lett.* **2003**, *381*, 766.

(43) Bilde, M.; Wallington, T. J.; Ferronato, G.; Orlando, J. J.; Tyndall, G. S.; Estupinan, E.; Haberkorn, S. *J. Phys. Chem. A* **1998**, *102*, 1976.

(44) Orkin, V. L.; Khamagonov, V. G.; Guschin, A. G.; Huie, R. E.; Kurylo, M. J. *J. Phys. Chem. A* **1997**, *101*, 174.

(45) Gillotay, D.; Jenouvrier, A.; Coquart, B.; Merienne, M. F.; Simon, P. C. *Planet. Space Sci.* **1989**, *37*, 1127.

(46) Tzeng, W. B.; Lee, Y. R.; Lin, S. M. *Chem. Phys. Lett.* **1994**, *227*, 467.

(47) McGivern, W. S.; Li, R.; Zou, P.; North, S. W. *J. Chem. Phys.* **1999**, *111*, 5771.

(48) Zou, P.; McGivern, W. S.; North, S. W. *Phys. Chem. Chem. Phys.* **2000**, *2*, 3785.

(49) Lee, S.-H.; Jung, Y.-J.; Jung, K.-H. *Chem. Phys.* **2000**, *260*, 143.

(50) Rozgonyi, T.; Feurer, T.; González, L. *Chem. Phys. Lett.* **2001**, *350*, 155.

(51) Orkin, V. L.; Kasimovskaya, E. E. *J. Atmos. Chem.* **1995**, *21*, 1.